

Vibration modes of a bubble close to a boundary

Jin-Ze Liu(刘金泽) and Wen-Shan Duan(段文山)

Citation: Chin. Phys. B, 2025, 34 (**5**): 054701. DOI: 10.1088/1674-1056/adbd24
http://cpb.iphy.ac.cn; http://iopscience.iop.org/cpb

What follows is a list of articles you may be interested in

Stable nanobubbles on ordered water monolayer near ionic model surfaces

Luyao Huang(黄璐瑶), Cheng Ling(凌澄), Limin Zhou(周利民), Wenlong Liang(梁文龙), Yujie Huang(黄雨婕), Lijuan Zhang(张立娟), Phornphimon Maitarad, Dengsong Zhang(张登松), and Chunlei Wang(王春雷)
Chin. Phys. B, 2025, 34 (**1**): 014701. DOI: 10.1088/1674-1056/ad989d

Dynamic modeling of cavitation bubble clusters: Effects of evaporation, condensation, and bubble—bubble interaction

Long Xu(许龙), Xin-Rui Yao(姚昕锐), and Yang Shen(沈阳)
Chin. Phys. B, 2024, 33 (**4**): 044702. DOI: 10.1088/1674-1056/ad181f

Simulation of single bubble dynamic process in pool boiling process under microgravity based on phase field method

Chang-Sheng Zhu(朱昶胜), Bo-Rui Zhao(赵博睿), Yao Lei(雷瑶), and Xiu-Ting Guo(郭秀婷)
Chin. Phys. B, 2023, 32 (**4**): 044702. DOI: 10.1088/1674-1056/aca209

Phase field simulation of single bubble behavior under an electric field

Chang-Sheng Zhu(朱昶胜), Dan Han(韩丹), Sheng Xu(徐升)
Chin. Phys. B, 2018, 27 (**9**): 094704. DOI: 10.1088/1674-1056/27/9/094704

Effect of supercritical water shell on cavitation bubble dynamics

Shao Wei-Hang (邵纬航), Chen Wei-Zhong (陈伟中)
Chin. Phys. B, 2015, 24 (**5**): 054701. DOI: 10.1088/1674-1056/24/5/054701

Vibration modes of a bubble close to a boundary

Jin-Ze Liu(刘金泽) and Wen-Shan Duan(段文山)[†]

College of Physics and Electronic Engineering, Northwest Normal University, Lanzhou 730070, China

(Received 27 November 2024; revised manuscript received 22 January 2025; accepted manuscript online 6 March 2025)

Using the recently proposed bubble equation, we study the vibration characteristics of a bubble close to a solid boundary. The results indicate that a rigid boundary has an important effect on large-amplitude bubble vibration. Whether the bubble vibration is stable or unstable strongly depends on the distance between the initial bubble center and the solid boundary. Furthermore, it also depends on both the amplitude and the frequency of the external perturbation. It is found that the smaller the distance between the initial bubble center and the solid boundary, the larger the initial bubble radius and the larger both the amplitude and frequency of the external perturbation, the more easily the bubble vibration becomes unstable. It is shown that this unstable bubble vibration is possibly related to the production of a reentrant microjet for the bubble, which suggests a potential method for estimating bubble size and the distance between the bubble center and the solid boundary by exerting an external perturbation with controllable amplitude and frequency on the liquid. Furthermore, the dependence of the natural frequency of the bubble on the external pressure for small-amplitude vibration can reveal the bubble radius and the distance between the bubble center and the solid boundary. In addition, the vibration characteristics of a bubble close to a solid boundary under a periodic external perturbation are revealed. Several bubble vibration modes are identified; the strongest vibration modes are those with the natural frequency and the external vibration frequency.

Keywords: bubble dynamics, spectral analysis

PACS: 47.55.dd, 43.25.+y

DOI: 10.1088/1674-1056/adbd24 **CSTR:** 32038.14.CPB.adbd24

1. Introduction

Rayleigh first studied cavitation and proposed a dynamical equation for bubbles[1]

$$R\ddot{R}+\frac{3}{2}\dot{R}^2=\frac{p_{\rm i}-p_\infty-\frac{2\sigma}{R}-\frac{4\mu}{R}\dot{R}}{\rho}, \tag{1}$$

where ρ represents the liquid density, $p_{\rm i}$ is the pressure inside the bubble, p_∞ is the pressure in the liquid far away from the bubble, σ represents the surface tension and μ is the coefficient of liquid viscosity. The equilibrium radius of the bubble, denoted by R_0, is given by $R_0=\frac{2\sigma}{p_{\rm i}-p_\infty}$ when the values of $p_{\rm i}$ and p_∞ are known, although this equilibrium state is unstable. It is important to note that Eq. (1) is derived under the assumptions of an incompressible liquid and isothermal compression of the gas within the bubble.

Two distinct approaches can be used to study bubbles: the first involves a permanent gas within the bubble, while the second involves the vapor of the surrounding liquid.[2,3] The focus of this investigation is on the first case, where the gas inside the bubble consists of a permanent gas.

Minnaert conducted a study on the linearized oscillations of a permanent gas bubble in a liquid as early as 1933.[4] Subsequent detailed investigations on this topic were conducted by other researchers.[5,6] Assuming a polytropic law of gas compression,[6,7] the natural frequency of the bubble can be determined.

The radial motion of a spherical bubble in a compressible liquid with no boundaries had already been investigated as early as the 19th century,[8] with subsequent studies on similar topics being conducted.[9,10] Keller and his colleagues derived the equation describing the radial motion of a spherical bubble in a compressible fluid as follows:[10,11]

$$\begin{aligned}&\left(1-\frac{\dot{R}}{c_\infty}\right)R\ddot{R}+\frac{3}{2}\left(1-\frac{\dot{R}}{3c_\infty}\right)(\dot{R})^2\\&=\frac{1}{\rho_\infty}\left(1+\frac{\dot{R}}{c_\infty}\right)[p_{\rm B}-p_\infty-p_{\rm v}]+\frac{R}{\rho_\infty c_\infty}\dot{p}_{\rm B}.\end{aligned} \tag{2}$$

The variable part of the pressure in the liquid at the location of the bubble center, in the absence of the bubble, is denoted by $p_{\rm v}=p_{\rm v}(t+\frac{R}{c_\infty})$, while $p_{\rm B}=p_{\rm B}(t)$ represents the pressure inside the bubble. Note that this equation is accurate to the first order in the Mach number of the bubble–wall motion. In the case where $c_\infty\to\infty$, this equation simplifies to the well-known Rayleigh–Plesset equation for incompressible bubble dynamics. The equation governing the radial motion of the bubble is given by

$$R\ddot{R}+\frac{3}{2}\dot{R}^2=\frac{p_{\rm i}-p_\infty-p_{\rm v}}{\rho_\infty}. \tag{3}$$

In 1986, Prosperetti and Lezzi proposed a similar equation to Eq. (2) using the perturbation method with respect to the bubble–wall Mach number.[12] The equation can be written

[†]Corresponding author. E-mail: duanws@nwnu.edu.cn

© 2025 Chinese Physical Society and IOP Publishing Ltd. All rights, including for text and data mining, AI training, and similar technologies, are reserved.

as

$$\left(1-\frac{\dot{R}}{c_\infty}\right)R\ddot{R}+\frac{3}{2}\left(1-\frac{\dot{R}}{3c_\infty}\right)(\dot{R})^2 = \left(1+\frac{\dot{R}}{c_\infty}+\frac{R}{c_\infty}\frac{\mathrm{d}}{\mathrm{d}t}\right)(h_\mathrm{B}-\frac{p(t)-p_\infty}{\rho_\infty}), \tag{4}$$

where $h_\mathrm{B}=\frac{p_\mathrm{B}-p_\infty}{\rho_\infty}$, $p(t)$ is also the liquid pressure at the bubble site in the absence of the bubble. It should be noted that when $p_\mathrm{v}(t+\frac{R}{c_\infty})\approx p_\mathrm{v}+\frac{R}{c_\infty}\frac{\mathrm{d}p_\mathrm{v}}{\mathrm{d}t}$, Eq. (4) reduces to Eq. (2). Therefore, Eqs. (4) and (2) are almost equivalent.

Herring[8] and Trilling[13] also proposed similar equations, given as follows:

$$\left(1-\frac{2\dot{R}}{c_\infty}\right)R\ddot{R}+\frac{3}{2}\left(1-\frac{4\dot{R}}{3c_\infty}\right)(\dot{R})^2 = \frac{1}{\rho_\infty}\left[p_\mathrm{B}(t)-p_\infty-p_\mathrm{v}\left(t+\frac{R}{c_\infty}\right)+\frac{R}{c_\infty}\frac{\mathrm{d}p_\mathrm{B}(t)}{\mathrm{d}t}\right]. \tag{5}$$

Mathematically speaking, Eqs. (2), (4) and (5) are equivalent in the limiting case when $(\dot{R}/c_\infty)^2$ is extremely small.

When subjected to external pressure, bubbles can either expand or contract periodically.[14–18] Conversely, when a bubble is in proximity to a solid boundary, certain parts of the bubble will contract at a faster rate, potentially leading to the formation of a reentrant jet capable of reaching speeds up to hundreds of meters per second.[19–25] This high-velocity jet poses a risk of damaging nearby solid surfaces.[26–31] Consequently, numerous researchers have focused their attention on understanding the dynamic characteristics of bubbles near solid boundaries.[32–37] Furthermore, a significant number of experimental studies have been conducted in this area.[38–46] Additionally, the dynamic properties of cavitation bubbles find various applications such as stone comminution in ultrasound lithotripsy,[47–49] surface cleaning,[50,51] ultrasonic contrast imaging,[52] drug delivery,[53–55] sonoporation in cells[56] and, in certain conditions, the potential to cause severe damage to target vessels.[57–60]

However, theoretical investigations into bubble vibration as well as related phenomena such as the reentrant microjet when a bubble is close to a solid boundary are still lacking in the current literature. Recently, a bubble dynamical equation was proposed to study this kind of problem.[61] This equation provides insights into the influence of a nearby solid boundary on a bubble's behavior,

Based on this equation,[61] the vibration characteristics of the bubble close to a solid boundary are studied in the present paper. The results show that the solid boundary has an important effect on large-amplitude bubble vibration. Whether the bubble vibration is stable or not strongly depends on the distance from the initial bubble center to the solid boundary (the initial bubble radius). It also depends on both the amplitude and the frequency of the external perturbation. The dependence of the stable region on the distance from the initial bubble center to the solid boundary as well as both the amplitude and the frequency of the external perturbation are shown in the present paper. Because unstable bubble vibration may result in a reentrant microjet for a bubble, a potential method for estimating the bubble size and the distance between the bubble center and the solid boundary is inferred. Therefore, by exerting an external perturbation with controllable amplitude and frequency on the liquid, and measuring the condition of the unstable bubble vibration or the condition of producing the reentrant microjet, we can estimate the bubble size and the distance between the bubble center and the solid boundary.

2. Model

This paper aims to investigate the small-amplitude oscillation of a bubble in the vicinity of a solid boundary under the influence of disturbance from external vibrations. In order to simplify the analysis and facilitate understanding, several assumptions are made: the boundary is considered to be an infinite plane and the liquid is assumed to be inviscid and irrotational.[62–64] To establish the coordinate system, a spherical coordinate (r,θ) is utilized, with the origin positioned at the center of the bubble and the positive z axis aligned parallel to the normal vector of the plane. In the assumed two-dimensional axisymmetric model, computational complexity is significantly reduced, while the vibration behavior of bubbles under symmetric conditions is effectively simulated. Specific applications include simulating the vibration and behavior of bubbles in a sound field, which is beneficial for designing efficient ultrasonic cleaning devices and acoustically driven microfluidic devices.[65,66] Additionally, this model can be used in medical ultrasound to simulate the behavior of bubbles under the action of ultrasound, thereby aiding in the improvement of ultrasound contrast agents and ultrasound therapies, among other applications.[67,68]

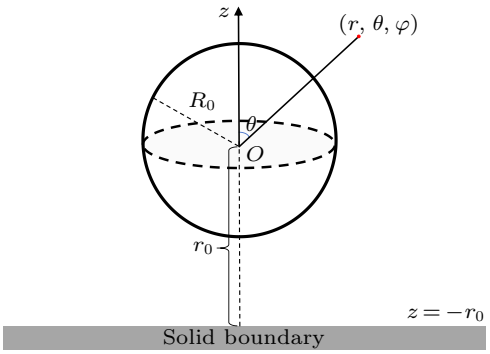


Fig. 1. Schematic view of the coordinate systems used in the model. The initial bubble radius is R_0, the distance between bubble center and the solid boundary is r_0, the solid boundary equation is $z=-r_0$.[61]

Then the bubble equation in dimensional form is as follows:[61,69]

$$R\ddot{R}\left\{1+\delta\left(1-\frac{\sin\theta}{r_0}R'\right)-\frac{2}{c_0}\dot{R}\right.$$

$$+\delta^2\left[-2\cos\theta+\frac{\sin\theta}{r_0}R'(3\cos\theta-1)+\frac{\sin^2\theta}{r_0^2}(R')^2\right]\Bigg\}$$
$$+(\dot{R})^2\left\{\frac{3}{2}+\delta\left(2-\frac{\sin\theta}{r_0}R'\right)-\frac{2}{c_0}\dot{R}\right.$$
$$\left.+\delta^2\left[-4\cos\theta+\frac{\sin\theta}{r_0}R'(3\cos\theta-2)+\frac{\sin^2\theta}{2r_0^2}(R')^2\right]\right\}$$
$$=h_{\rm B}-\frac{p_{\rm v}}{\rho_0}+\frac{1}{c_0}R\dot{h}_{\rm B}, \tag{6}$$

where $R=R(\theta,t)$ is the bubble radius with R_0 the initial value at equilibrium, $\delta=R_0/r_0$, where r_0 represents the distance between the initial bubble center and the solid boundary, c_0 is the acoustic speed of the liquid, $h_{\rm B}=p_{\rm B}/\rho_0$, $p_{\rm B}$ is the liquid pressure close to the interface between liquid and the bubble, ρ_0 is the liquid density, $\dot{R}=\partial R/\partial t$ and $R'=\partial R/\partial\theta$ are the derivatives of R with respect to t and θ, respectively, and θ is the angle between the positive z direction and the vector from the origin of the coordinate to the point of consideration (see Fig. 1). In Eq. (6), $p_{\rm v}=p_\infty+p'_{\rm v}$ is the liquid pressure, where p_∞ is the liquid pressure when the distance between bubble center to the point being considered is large enough, $p'_{\rm v}$ represents the variable part of the pressure in the liquid at the location of the bubble center in the absence of the bubble. The equation for the solid boundary is given by $z=-r_0$.

By neglecting the effect of the boundary, i.e., as δ approaches 0, Eq. (6) simplifies to

$$R\ddot{R}\left(1-\frac{2}{c_0}\dot{R}\right)+(\dot{R})^2\left(\frac{3}{2}-\frac{2}{c_0}\dot{R}\right)=h_{\rm B}-\frac{p_{\rm v}}{\rho_0}+\frac{1}{c_0}R\dot{h}_{\rm B}. \tag{7}$$

Equation (7) is Eq. (5) in this limit case. It indicates that Eq. (6) is reliable.

3. Oscillation of the bubble close to a solid boundary under external harmonic vibration

3.1. Natural oscillation and frequency of the bubble

When the bubble is compressed by the inertia of the inrushing liquid due to the perturbed external pressure, both the pressure and temperature of the gas inside the bubble change rapidly. It is reasonable to assume that the gas inside the bubble behaves adiabatically, represented by the equation $p_{\rm gas0}V_{\rm gas0}^{\gamma}=p_{\rm gas}V_{\rm gas}^{\gamma}$, where $p_{\rm gas0}$ is the initial gas pressure, $\gamma=1.4$,[70] $V_{\rm gas}=\frac{2}{3}\int_0^\pi\sin\theta R(t,\theta){\rm d}\theta$ represents the bubble volume and $V_{\rm gas0}=\frac{4\pi}{3}R_0^3$ represents the initial bubble volume.

When external disturbances are present, the bubble will either vibrate or collapse. The motion of the bubble is described by Eq. (6). To determine the bubble's natural oscillation and its frequency, an approximate equation is now presented based on Eq. (6). The following equation is derived under the limited conditions of linear approximation and a sufficiently small value of δ:

$$\ddot{R}+\frac{3}{2}\frac{\dot{R}^2}{R}+\frac{p_{\rm v}-p_{\rm B}}{\rho_0R^2}R=0. \tag{8}$$

Equation (8) provides an estimation of the natural frequency of a bubble when the solid boundary is sufficiently distant from the bubble as follows:

$$\omega_{\rm N}=\left(\frac{p_{\rm v}-p_{\rm B}}{\rho_0R^2}\right)^{\frac{1}{2}}. \tag{9}$$

In the following, we will estimate the natural frequency of a bubble in water. Assuming a liquid pressure of $p_{\rm v}=1.1\times10^5$ Pa and a bubble pressure of $p_{\rm B}=1.0\times10^5$ Pa, the natural frequency of a bubble is estimated to be $\omega_{\rm N}\sim2.0\times10^5$ rad/s, considering the surface tension coefficient of water as $\sigma=0.073$ N/m and the bubble radius as approximately $R_0\approx1.46\times10^{-5}$ m. The equation $p_{\rm v}=p_{\rm B}+\frac{2\sigma}{R}$ is used.

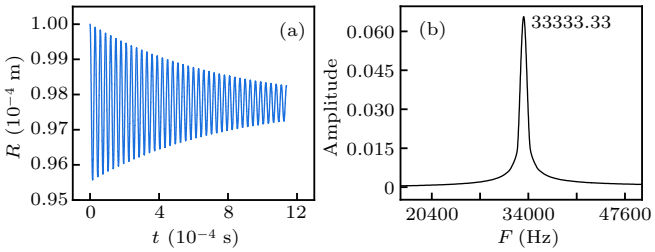


Fig. 2. (a) Dependence of the bubble radius on time at $\theta=0°$, 90° and 180°. The three curves coincide due to the negligible boundary effect, with the following parameter values: $\delta=1.0\times10^{-7}$, $R_0=1.0\times10^{-4}$ m, $p_{\rm v}=1.1\times10^5$ Pa, $p_{\rm B}=1.0\times10^5$ Pa. (b) The Fourier frequency analysis of the bubble vibration, corresponding to (a). Amp is the amplitude of vibration.

To verify the accuracy of our estimation of the natural frequency of a bubble, we numerically solve Eq. (6) with the given initial conditions: $\delta=1.0\times10^{-7}$, $R_0=1.0\times10^{-4}$ m, $p_{\rm v}=1.1\times10^5$ Pa and $p_{\rm B}=1.0\times10^5$ Pa. The dependence of the bubble radius at $\theta=0°$, 90° and 180° on time is shown in Fig. 2(a). Additionally, the Fourier frequency analysis of the bubble's vibration is presented in Fig. 2(b). Our findings indicate that the relative deviation between the approximated analytical natural frequency of the bubble and the corresponding numerical one is below 3%, indicating that both are in good agreement.

However, there is a question regarding the accuracy of the natural frequency of a bubble as calculated by Eq. (8) when the bubble is close to the solid boundary. To address this concern, numerical results obtained by solving Eq. (6) are provided. Figure 3 shows the dependence of the analytical natural frequency on the parameter δ. Notice that the natural frequency of a bubble decreases as the bubble center becomes close to the solid boundary. The fitted result for the bubble natural frequency from the numerical simulation is $f_{\rm N}=f_\infty\delta^{-0.0043}$, where f_∞ represents the natural frequency of the bubble when the bubble is sufficiently far from the solid boundary, $f_\infty\approx3.1\times10^4$ Hz, where the other parameters are $p_{\rm v}=1.1\times10^5$ Pa, $p_{\rm B}=1.0\times10^5$ Pa and $R_0=1.0\times10^{-4}$ m.

More numerical results demonstrate that the bubble vibration frequency also depends on other quantities such as r_0, R_0

and p_v. In the following, we try to find the dependence of the bubble vibration frequency on the parameters r_0, R_0 and p_v.

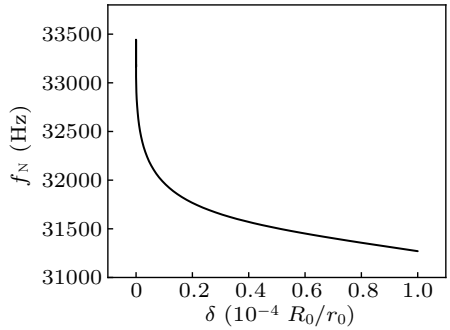


Fig. 3. (a) Dependence of the natural frequency of a bubble on the parameter $\delta = R_0/r_0$, where the other parameters are $R_0 = 1.0\times10^{-4}$ m, $p_v = 1.1\times10^5$ Pa and $p_B = 1.0\times10^5$ Pa.

The numerical results for the dependence of the natural frequency of the bubble (f_N) on R_0 and r_0 when p_v is fixed are given in Fig. 4. The fitted result for Fig. 4 is as follows:

$$\begin{aligned} f_N = {} & 1.113\times10^4 - 29.3r_0 - 4.6\times10^6 R_0 + 4.4\times10^{-2} r_0^2 \\ & - 1799 r_0 R_0 - 6.48\times10^9 R_0^2 \\ & - 2.3\times10^{-5} r_0^3 - 0.68 r_0^2 R_0 \\ & + 1.8\times10^6 r_0 R_0^2 + 3.08\times10^{12} R_0^3. \end{aligned} \tag{10}$$

Both Fig. 4 and Eq. (10) indicate that the natural frequency of the bubble decreases as its radius increases, while it exhibits almost no dependence on the parameter r_0, although it slightly increases with increasing r_0.

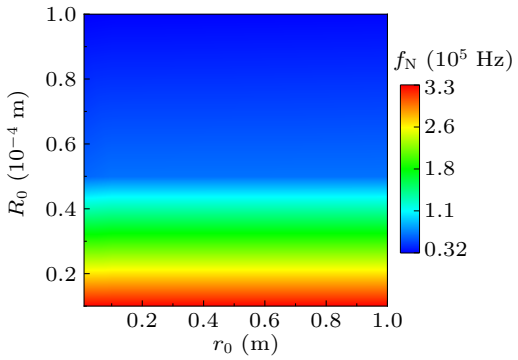


Fig. 4. Dependence of the natural frequency of a bubble on the parameters of both R_0 and r_0, where the other parameters are $p_v = 1.1\times10^5$ Pa and $p_B = 1.0\times10^5$ Pa.

Similarly, the numerical results for the dependence of the natural frequency of the bubble (f_N) on R_0 and p_v when r_0 is fixed are given in Fig. 5. The fitted result for Fig. 5 is as follows:

$$\begin{aligned} f_N = {} & 1.135\times10^5 + 0.8511 p_v - 1.081\times10^{-9} R_0 \\ & - 6.51\times10^{-7} p_v^2 - 2251 p_v R_0 + 2.417\times10^{12} R_0^2 \\ & + 2.389\times10^{-13} p_v^3 + 6.75\times10^{-4} p_v^2 R_0 \\ & - 1.489\times10^6 p_v R_0^2 - 1.5\times10^{15} R_0^3. \end{aligned} \tag{11}$$

The numerical results indicate that the natural frequency of the bubble increases as external pressure increases, while it decreases as the bubble radius increases. However, the natural frequency is nearly independent of the distance between the bubble center and the solid boundary, although it exhibits a weak increase as this increases.

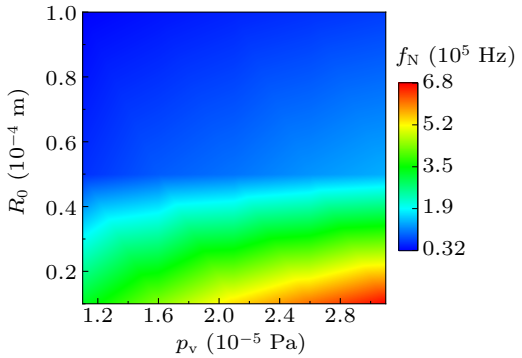


Fig. 5. Dependence of the natural frequency of a bubble on the parameters R_0 and p_v, where the other parameters are $r_0 = 10$ m and $p_B = 1.0\times10^5$ Pa.

3.2. Bubble vibrations under external periodic perturbations

In this section we aim to investigate the vibration characteristics of a bubble subjected to external periodic perturbations in a liquid. To achieve this, we assume that there are external perturbations to the liquid pressure given by the following equation:

$$p_v = p_0 + a_0 \cos(2\pi f_0 t + \phi), \tag{12}$$

where p_0 represents the pressure of the liquid in an infinite space, a_0 denotes the amplitude of the external pressure vibration, f_0 represents the frequency of the external pressure vibration and ϕ denotes the initial phase.

Figure 6(a) show the numerical results obtained from Eq. (6), which illustrate the variation of the bubble radius at angles $\theta = 0°$, $90°$ and $180°$ with respect to time. The other fixed parameters are $f_0 = 0.5 f_N = 1.67\times10^4$ Hz, where $f_N = 3.3\times10^4$ Hz, $a_0 = 1.0\times10^4$ Pa, $\phi = 0$, $p_0 = 1.0\times10^5$ Pa, $p_B = 1.0\times10^5$ Pa, $\delta = 1.0\times10^{-7}$ and $R_0 = 1.0\times10^{-4}$ m.

It is observed from Fig. 6(a) that the bubble exhibits quasi-periodic vibration. Figure 6(b) shows the corresponding Fourier frequency analysis, which reveals three frequencies associated with the bubble's vibration. These frequencies include the external perturbation frequency $f_0 = 1.67\times10^4$ Hz, the bubble's natural frequency $f_N = 3.3\times10^4$ Hz and a third frequency which is approximately the summation of two frequencies 5×10^4 Hz.

To further investigate, we vary the external perturbation frequency f_0 in order to observe the bubble's vibration characteristics. For this purpose, we select $f_0 = 3.3\times10^4$ Hz, which is approximately the analytical result of the bubble's natural frequency. However, the numerical result shows that the natural frequency of the bubble vibration is $f_N = 31146$ Hz, which slightly differs from the analytical result.

The dependence of the bubble radius at $\theta = 0°$, $90°$ and $180°$ on time are shown in Fig. 6(c). The other parameters are the same as those in Fig. 6(a). Figure 6(c) shows that the bubble also exhibits quasi-periodic vibration. By analyzing the Fourier frequency spectrum presented in Fig. 6(d), we observe that the bubble vibration comprises six frequencies: $f_1 = 2633$ Hz, $f_2 = 32796$ Hz, $f_3 = 64226$ Hz, $f_4 = 97022$ Hz, $f_5 = 129819$ Hz and $f_6 = 161249$ Hz.

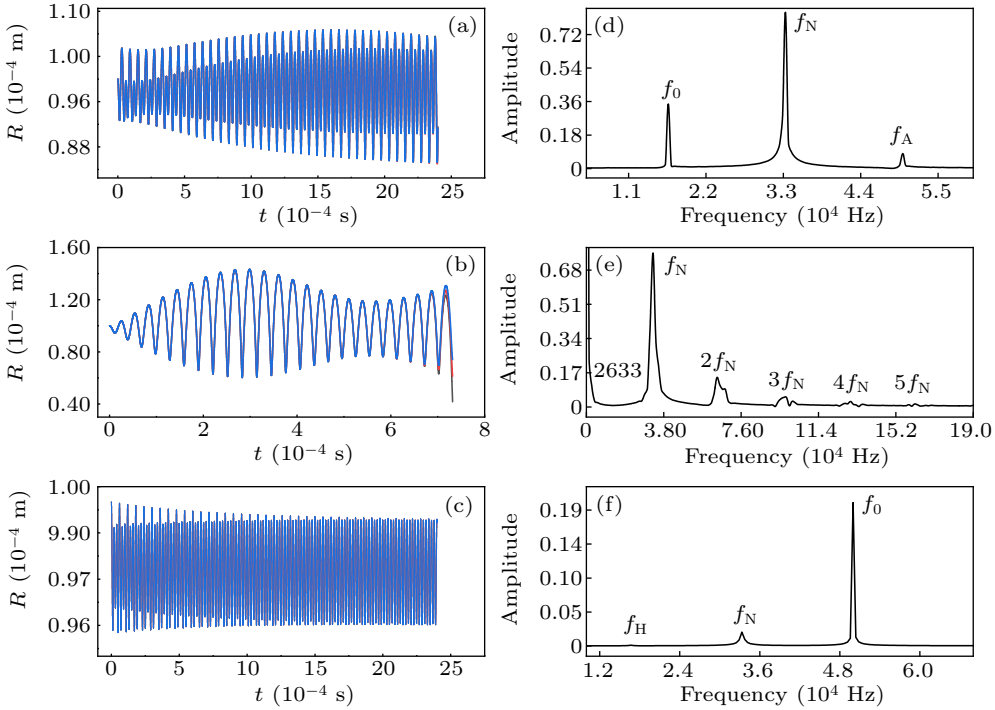


Fig. 6. The fixed simulation parameters are as follows: $f_N = 3.3 \times 10^4$ Hz (the natural frequency of the bubble), $a_0 = 1.0 \times 10^4$ Pa, $\phi = 0$, $p_0 = p_B = 1.0 \times 10^5$ Pa, $\delta = 1.0 \times 10^{-7}$, $R_0 = 1.0 \times 10^{-4}$ m. (a) Dependence of the bubble radius at $\theta = 0°$, $90°$ and $180°$ on time, with driving frequency $f_0 = 0.5 f_N = 1.67 \times 10^4$ Hz. (b) Fourier frequency analysis of the bubble vibration, corresponding to (a). (c) Dependence of the bubble radius at $\theta = 0°$, $90°$ and $180°$ on the time, but with $f_0 = f_N = 3.3 \times 10^4$ Hz. (d) Fourier frequency analysis of the bubble vibration, corresponding to (c). (e) Dependence of the bubble radius at $\theta = 0°$, $90°$ and $180°$ on time, but with $f_0 = 5.0 \times 10^4$ Hz. (f) Fourier frequency analysis of the bubble vibration, corresponding to (e).

It is widely known that linear superposition of two distinct linear vibrations with different frequencies, amplitudes and initial phases, denoted by $x_1 = A_1 \cos(2\pi f_a t + \varphi_1)$ and $x_2 = A_2 \cos(2\pi f_b t + \varphi_2)$, yields new vibration as follows: $x = x_1 + x_2 = A\cos(2\pi f t + \varphi)$, where

$$A = \sqrt{A_1^2 + A_2^2 + 2A_1A_2\cos[2\pi(f_b - f_a)t + \varphi_2 - \varphi_1]},$$
$$f = \frac{A_1^2 2\pi f_a + A_2^2 2\pi f_b + A_1A_2(2\pi f_a + 2\pi f_b)\cos[(2\pi f_b - 2\pi f_a)t + (\varphi_2 - \varphi_1)]}{2\pi\left(A_1^2 + A_2^2 + 2A_1A_2\cos(2\pi f_b - 2\pi f_a)t + (\varphi_2 - \varphi_1)\right)}, \quad \varphi = \arctan\frac{A_1\sin\varphi_1 + A_2\sin\varphi_2}{A_1\cos\varphi_1 + A_2\cos\varphi_2}.$$

For the special case $A_1 = A_2, \varphi_1 = \varphi_2 = 0$, $f_a = 31146$ Hz (the natural frequency of the bubble), $f_b = 33333$ Hz (the external disturbance frequency). The bubble vibration produces two frequencies. One frequency is the beat frequency of 2187 Hz and the other frequency is 32239 Hz.

These six frequencies can be explained as follows: f_1 represents the beat frequency produced by the combination of the natural frequency and perturbation frequency. f_2 corresponds to the perturbation frequency. The remaining frequencies, f_3, f_4, f_5 and f_6, are the harmonic frequencies of the bubble's natural frequency.

When the external perturbation frequency is $f_0 = 5.0 \times 10^4$ Hz, Fig. 6(e) indicates that the bubble vibration is also quasi-periodic. The Fourier frequency analysis in Fig. 6(f) reveals the presence of three distinct vibration frequencies. The first frequency corresponds to the external perturbation frequency of $f_0 = 5.0 \times 10^4$ Hz, the second frequency corresponds to the natural frequency of $f_N = 3.33 \times 10^4$ Hz and the third frequency is $f_H = 1.67 \times 10^4$ Hz, which is exactly half the natural frequency of the bubble.

The results indicate that the bubble exhibits different vibration modes depending on the external disturbances, particularly their frequency. To gain a better understanding of how external vibrations affect the characteristics of bubble vibration, Fig. 7 shows the variations of the bubble vibration frequencies (f_{an}) with respect to the external perturbed frequency (f_0). Notice from Fig. 7 that multiple frequencies of bubble vibration can be observed, including f_{1n}, f_2, f_3, f_4 and so on,

where $f_{1n} = nf_{\rm N}$. Here, $f_{\rm N}$ represents the natural frequency of the bubble, with $n = 1, 2, 3, \ldots$.

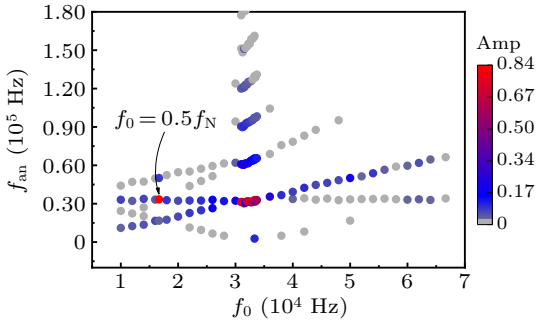


Fig. 7. Dependence of the bubble vibration frequency $f_{\rm an}$ on the external perturbation frequency f_0, where the colors represent the strength of the corresponding vibration mode, the other parameters are $R_0 = 1.0 \times 10^{-4}$ m, $r_0 = 100$ m, $p_0 = 1.0 \times 10^5$ Pa, $p_{\rm B} = 1.0 \times 10^5$ Pa, $a_0 = 1.0 \times 10^4$ Pa and $\phi = 0$.

First, it appears that there are multiple higher-order harmonic frequencies of the bubble vibration. Additionally, the fundamental frequency ($n = 1$) appears to be the dominant vibration mode of the bubble. As the value of the parameter n increases, its strength decreases.

Second, f_2 is equivalent to $f_{\rm N}$ and $f_{\rm N}/2$. This suggests the existence of a bubble vibration mode with a frequency that matches the natural frequency of the bubble. It is observed that the strongest vibration modes occur when $f_0 \approx f_{\rm N}$ and the second strongest one is when $f_0 \approx f_{\rm N}/2$.

Third, f_3 is equal to f_0, which is the frequency of the external disturbance. This indicates the existence of a bubble vibration mode that matches the frequency of the external disturbance.

Fourth, f_4 is equal to $2f_0$. This suggests the presence of a bubble vibration mode that exhibits a frequency approximately twice that of the external disturbance.

Fifth, within the range $0 \le f_0 \le f_{\rm N}$, $f_5 = f_{\rm N} - f_0$. Within the range $f_{\rm N} \le f_0 \le 2f_{\rm N}$, $f_5 = f_0 - f_{\rm N}$.

Last, within the range $0 \le f_0 \le f_{\rm N}$, $f_6 = f_{\rm N} + f_0$.

Figure 7 shows the dependence of the bubble vibration frequencies and their corresponding strengths on the external perturbation frequency. For better understanding, the dependence of the bubble vibration frequencies and their corresponding strengths on the distance from the bubble center to the solid boundary r_0 is given in Fig. 8.

Figures 8(a)–8(d) show the dependence of the power amplitude of the bubble vibration on both the distance from the bubble center to the solid boundary, r_0, and the bubble vibration frequency, $f_{\rm an}$, where the external perturbation frequency $f_0 = 0.5f_{\rm N}$, $f_{\rm N}$, $1.5f_{\rm N}$ and $2f_{\rm N}$, respectively, where $f_{\rm N} = 3.33 \times 10^4$ Hz. The other parameters for these four figures are fixed (see Fig. 8). It is inferred from Fig. 8 that the impact of the distance between the bubble center and the solid boundary on bubble vibration is not apparent. However, the external vibration frequency has a strong effect on the strength or the amplitude of the bubble vibration.

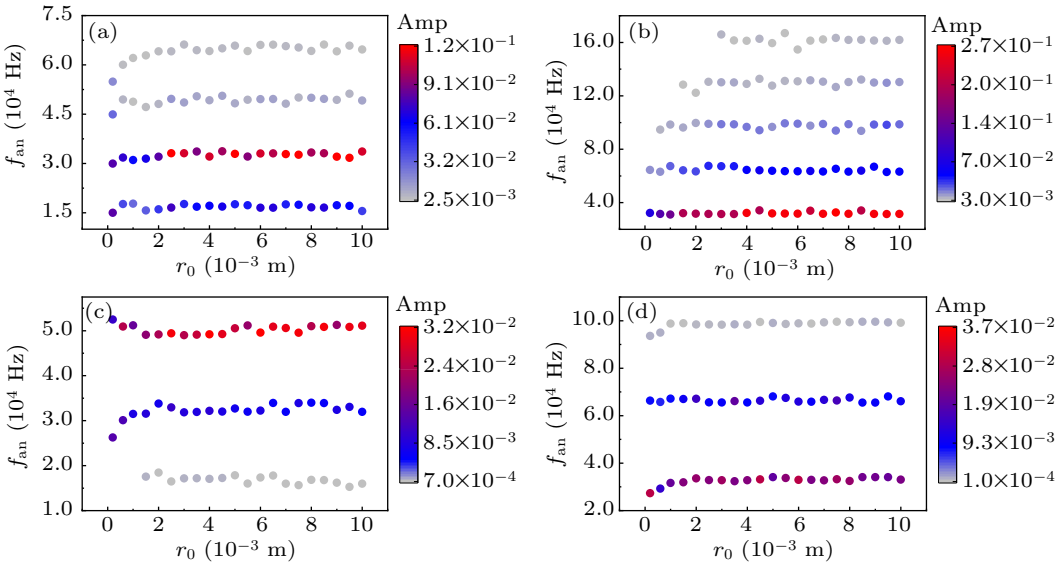


Fig. 8. Dependence of the power amplitude of the bubble vibration on the distance from the bubble center to the solid boundary (r_0) and the bubble vibration frequency ($f_{\rm an}$). The fixed simulation parameters are as follows: $R_0 = 1.0 \times 10^{-4}$ m, $p_0 = 1.0 \times 10^5$ Pa, $p_{\rm B} = 1.0 \times 10^5$ Pa, $a_0 = 1.0 \times 10^4$ Pa and $\phi = 0$. (a) The external perturbation frequency f_0 is half the natural frequency of the bubble vibration $f_{\rm N}$, i.e., $f_0 = 0.5f_{\rm N} = 1.67 \times 10^4$ Hz. (b) $f_0 = f_{\rm N} = 3.33 \times 10^4$ Hz. (c) $f_0 = 1.5f_{\rm N} = 5 \times 10^4$ Hz. (d) $f_0 = 2f_{\rm N} = 6.67 \times 10^4$ Hz.

3.3. Large-amplitude oscillation of the bubble

The numerical results show that the bubble vibration becomes asymmetric when either the initial bubble center is close enough to the solid boundary or when the external perturbation amplitude is large enough. In this case, the bubble radius depends not only on the time but also on the parameter θ during its vibration when there is a solid boundary.

Figure 9(a) shows the bubble cross section shape at different times $t = 0$ s, 4.5×10^{-5} s, 8.3×10^{-5} s and 1.3×10^{-4} s,

respectively, where $p_0 = 1.0 \times 10^5$ Pa, $p_B = 1.0 \times 10^5$ Pa, $a_0 = 10^4$ Pa, $\omega = 3.3 \times 10^4$ rad/s, $\phi = 0$, $R_0 = 10^{-4}$ m, $r_0 = 2.0 \times 10^{-4}$ m and $\dot{R}_0 = 0$ m/s.

It should be noted that the bubble radius depends on both time and the parameter θ. For further understanding, the corresponding variations of the bubble radius $R(\theta,t)$ with respect to time t for different parameters of $\theta = 0°$, 90° and 180° are shown in Fig. 9(b). It is observed from Fig. 9(b) that the bubble radius at $\theta = 0°$ becomes much smaller than those at the other regions. Figure 9(c) shows the dependence of the velocity of the bubble interface, $\dot{R}(\theta,t)$, on time t for $\theta = 0°$, 90° and 180°, respectively.

It is evident from Fig. 9(c) that the velocity of the bubble interface, $\dot{R}(\theta,t)$, depends on the parameter θ. Moreover, Fig. 9(d) shows the dependence of $\Delta\dot{R} = \dot{R}(0°,t) - \dot{R}(180°,t)$ and $\Delta\dot{R} = \dot{R}(90°,t) - \dot{R}(180°,t)$ on time t. It seems from Fig. 9(d) that the difference in the velocity of the bubble interface between $\theta = 0°$ and $\theta = 180°$ increases rapidly with time.

It seems that as $\Delta\dot{R} = \dot{R}(0°,t) - \dot{R}(180°,t)$ increases, the bubble vibration become unstable. In this case, a liquid jet can possibly be produced. Suppose that if $\Delta\dot{R} = \dot{R}(0°,t) - \dot{R}(180°,t) > v_C$ the bubble vibration is unstable, which may be related to the production of the liquid jet. The dependence of v_C on the system parameters may be a subject for our future work.

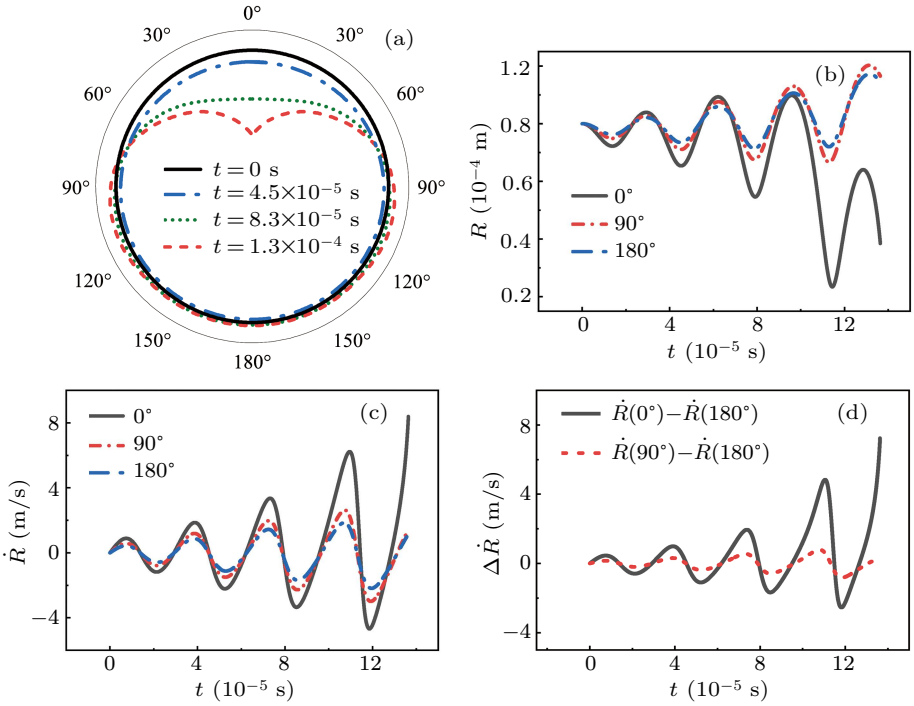


Fig. 9. (a) Bubble cross-section shape at time $t = 0$ s, 4.5×10^{-5} s, 8.3×10^{-5} s, 1.3×10^{-4} s respectively, where $p_0 = 1.0 \times 10^5$ Pa, $p_B = 1.0 \times 10^5$ Pa, $a_0 = 10^4$ Pa, $\omega = 3.3 \times 10^4$ rad/s, $\phi = 0$, $R_0 = 10^{-4}$ m, $r_0 = 2.0 \times 10^{-4}$ m and $\dot{R}_0 = 0$ m/s. (b) The variation of the bubble radius $R(\theta,t)$ with respect to time t for $\theta = 0°$, 90° and 180° respectively. (c) The variation of the velocity of the bubble interface, $\dot{R}(\theta,t)$, for $\theta = 0°$, 90° and 180°, respectively. (d) The variation of the velocity differences of the bubble interface between two points: $\Delta\dot{R} = \dot{R}(0°,t) - \dot{R}(180°,t)$ and $\Delta\dot{R} = \dot{R}(90°,t) - \dot{R}(180°,t)$ with respect to time.

4. Conclusion

Based on the recently proposed bubble equation, we conducted an investigation on the vibration characteristics of a bubble close to a solid boundary. The results indicate that the natural frequency of the bubble increases with increase in the external pressure for small-amplitude vibration, while it decreases as the bubble radius increases. However, it shows that there is only a weak increase in the natural frequency with increase in the distance between the bubble center and the solid boundary.

In addition, the vibration characteristics of a bubble close to a solid boundary under a periodic external perturbation are revealed. Several bubble vibration modes are identified, for example, the higher-order harmonic natural frequencies of the bubble vibration, the vibration mode with a frequency of either the natural frequency of the bubble or half of the natural frequency, a vibration mode with a frequency of either the external vibration frequency or twice the external vibration frequency, as well as a vibration mode with a frequency of both the sum and the difference of the external vibration frequency and the natural frequency of the bubble. The stronger vibration modes are those with either the natural frequency or the external vibration frequency.

The present paper found that the rigid boundary has an important effect on the large-amplitude bubble vibration, especially on whether the bubble vibration is stable or unstable. It is found that the bubble vibration is unstable if the amplitude of the external perturbation is large enough or if the frequency

of the external perturbation is large enough. Furthermore, the bubble vibration is unstable if either the bubble radius is large enough or if the distance between the bubble center and the solid boundary is small enough. It is found that unstable bubble vibration is possibly related to the production of a reentrant microjet for a bubble.

These results offer potential applications in various fields, such as ultrasound lithotripsy, ultrasonic cleaning and medical ultrasound therapies, where the control of bubble dynamics is essential. By modulating external perturbations, it may be possible to enhance energy transfer, improve cleaning efficiency and optimize therapeutic outcomes. Additionally, the proposed method of estimating bubble size and its distance from a boundary through controlled perturbations provides a novel approach for non-invasive diagnostics in fluid systems.

Acknowledgement

This work was supported by the National Natural Science Foundation of China (Grant No. 12275223).

References

[1] Plesset M S and Prosperetti A 1977 *Ann. Rev. Fluid Mech.* **9** 145
[2] PIesset M S 1949 *J. Appl. Mech.* **16** 277
[3] Brennen C 1973 *ASME. J. Fluids Eng.* **95** 533
[4] Minnaert M 1933 *Philos. Mag.* **16** 235
[5] Plesset M S and Hsieh D Y 1960 *Phys. Fluids* **3** 882
[6] Chapman R B and Plesset M S 1971 *J. Basic Eng.* **93** 373
[7] Devin C 1959 *J. Acoust. Soc. Am.* **31** 1654
[8] Brennen C E 2013 *Cavitation and Bubble Dynamics* (Cambridge University Press)
[9] Cole R H and Weller R 1948 *Phys. Today* **1** 35
[10] Keller J B and Kolodner I I 1956 *J. Appl. Phy.* **27** 1152
[11] Keller J B and Miksis M 1980 *J. Acouet. Soc. Am.* **68** 628
[12] Prosperetti A and Lezzi A 1986 *J. Fluid Mech.* **168** 457
[13] Trilling L 1952 *J. Appl. Phys.* **23** 14
[14] Magaletti F, Marino L and Casciola C M 2015 *Phys. Rev. Lett.* **114** 064501
[15] Koukouvinis P, Gavaises M, Supponen O and Farhat M 2016 *Phys. Fluids* **28** 052103
[16] Shaw S J and Spelt P D M 2010 *J. Fluid Mech.* **646** 363
[17] Brujan E A, Keen G S, Vogel A and Blake J R 2002 *Phys. Fluids* **14** 85
[18] Xu L, Yao X R and Shen Y 2024 *Chin. Phys. B* **33** 044702
[19] Karri B, Avila S R G, Loke Y C, O'Shea S J, Klaseboer E, Khoo B C and Ohl C D 2012 *Phys. Rev. E* **85** 015303
[20] Wang X L, Wang Y, Liu H L, Xiao Y D, Jiang L L and Li M 2023 *Int. J. Heat Mass Tran.* **201** 123591
[21] Zhao X T, Shen X, Geng L L, Zhang D S and Van Esch B P M 2023 *Phys. Fluids* **35** 115135
[22] Zhu C S, Zhao B R, Lei Y and Guo X T 2023 *Chin. Phys. B* **32** 044702
[23] Lindau O and Lauterborn W 2003 *J. Fluid Mech.* **479** 327
[24] Supponen O, Obreschkow D, Tinguely M, Kobel P, Dorsaz N and Farhat M 2016 *J. Fluid Mech.* **802** 263
[25] Hsiao C T, Jayaprakash A, Kapahi A, Choi J K and Chahine G L 2014 *J. Fluid Mech.* **755** 142
[26] Appel J, Koch P, Mettin R, Krefting D and Lauterborn W 2004 *Ultrason. Sonochem.* **11** 39
[27] Luo X W, Ji B and Tsujimoto Y 2016 *J. Hydrodyn.* **28** 335
[28] Philipp A and Lauterborn W 1998 *J. Fluid Mech.* **361** 75
[29] Luo J, Xu W L, Deng J, Zhai Y W and Zhang Q 2018 *Water* **10** 1262
[30] Sagar H J and Moctar O E 2020 *J. Fluids Struct.* **92** 102799
[31] Zhu S, Cocks F H, Preminger G M and Zhong P 2002 *Ultrasound Med. Biol.* **28** 661
[32] Brujan E A, Ikeda T and Matsumoto Y 2004 *Phys. Fluids* **16** 2402
[33] Ni B Y, Zhang A M and Wu G X 2015 *J. Fluid Eng.* **137** 031206
[34] Lauer E, Hu X Y, Hickel S and Adams N A 2012 *Comput. Fluids* **69** 1
[35] Li S M, Zhang A M, Wang Q X and Zhang S 2019 *Phys. Fluids* **31** 107105
[36] Koch M, Lechner C, Reuter F, Köhler K, Mettin R and Lauterborn W 2015 *Comput. Fluids* **126** 71
[37] Sagar H J and Moctor O E 2020 *J. Fluids Struct.* **92** 102799
[38] Oguchi K, Enoki M and Hirata N 2015 *Mater. Trans.* **56** 534
[39] Chen T N, Guo Z N, Zeng B W, Yin S H, Deng Y and Li H H 2017 *Int. Adv. Manuf. Technol.* **93** 3275
[40] Zhang Y N, Qiu X, Zhang X Q, Tao N N and Zhang Y N 2020 *Ultrason. Sonochem.* **67** 105157
[41] Wang C, Rallabandi B and Hilgenfeldt S 2013 *Phys. Fluids* **25** 02200
[42] Shaw S J, Jin Y H, Schiffers W P and Emmony D C 1996 *J. Acoust. Soc. Am.* **99** 2811
[43] Vesipa R, Paissoni E, Manes C and Ridolfi L 2021 *Phys. Rev. E* **103** 023108
[44] Han R, Tao L B, Zhang A M and Li S 2019 *Ocean Eng.* **186** 106096
[45] Cui P, Zhang A M, Wang S P and Liu Y L 2020 *J. Fluid Mech.* **897** A25
[46] Li X F, Duan Y X, Zhang Y N, Tang N N and Zhang Y N 2019 *Symmetry* **11** 1051
[47] Colonius T, Hagmeijer R, Ando K and Brennen C E 2008 *Phys. Fluids* **20** 040902
[48] Brujan E A, Ikeda T, Yoshinaka K and Matsumoto Y 2011 *Ultrason. Sonochem.* **18** 59
[49] Zhan S P, Duan H T, Pan L, Tu J S, Jia D, Yang T and Li J 2021 *Phys. Chem. Chem. Phys.* **23** 8446
[50] Trummler T, Bryngelson S H, Schmidmayer K, Schmidt S J, Colonius T and Adams N A 2020 *J. Fluid Mech.* **899** A16
[51] Tang H, Liu Y L, Cui P and Zhang A M 2020 *J. Hydrodyn.* **32** 1029
[52] Zhao R, Xu R Q, Shen Z H, Lu J and Ni X W 2007 *Opt. Laser Technol.* **39** 968
[53] Cui P, Zhang A M and Wang S P 2021 *Ocean Eng.* **234** 109175
[54] Cui J, Zhou T R, Huang X and Li Z C 2021 *Ultrason. Sonochem.* **75** 105587
[55] Chahine G L, Kapahi A, Choi J K and Hsiao C T 2016 *Ultrason. Sonochem.* **29** 528
[56] Ohl C D, Arora M, Dijkink R, Janve V and Lohse D 2006 *Appl. Phys. Lett.* **89** 074102
[57] Hung C F and Hwangfu J J 2010 *J. Fluid Mech.* **651** 55
[58] Brett J M and Yiannakopolous G 2008 *Int. J. Impact Eng.* **35** 206
[59] Klaseboer E, Hung K C, Wang C, Wang C W, Khoo B C, Boyce P, Debono S and Charlier H 2005 *J. Fluid Mech.* **537** 387
[60] Wu W, Liu M, Zhang A M and Liu Y L 2021 *Phys. Rev. Fluids* **6** 013605
[61] Liu J Z, Hong X R, Ma J K and Duan W S 2022 *Mod. Phys. Lett. B* **36** 2250133
[62] Taborda M A, Sommerfeld M and Muniz M 2021 *Chem. Eng. Sci.* **229** 116121
[63] Dehane A, Merouani S, Hamdaoui O and Alghyamah A 2021 *Ultrason. Sonochem.* **73** 105498
[64] Omoteso K A, Roy-Layinde T O, Laoye J A, Vincent U E and McClintock P V E 2021 *Ultrason. Sonochem.* **70** 105346
[65] Miyauchi T and Takata S 2024 *Phys. Rev. E* **110** 025102
[66] Xu P, Li B, Ren Z B, Liu S H and Zuo Z G 2023 *Phys. Rev. Fluids* **8** 083601
[67] Feng K, Eshraghi J, Vlachos P P and Gomez H 2024 *Phys. Fluids* **36** 053305
[68] Shaw S J 2006 *Phys. Fluids* **18** 072104
[69] Liu J Z and Duan W S 2024 *Indian J. Phys.* **98** 2105
[70] Gvozdeva L, Gavrenkov S and Nesterov A 2015 *Shock Waves* **25** 283